FusionU-Net: U-Net with Enhanced Skip Connection for Pathology Image Segmentation

Zongyi Li, Hongbing Lyu
Zhejiang University
Hangzhou, China
{zongyi_li, lhb}@zju.edu.cn

Jun Wang
Hangzhou City University
Hangzhou, China
wjcy19870122@163.com

ABSTRACT

In recent years, U-Net and its variants have been widely used in pathology image segmentation tasks. One of the key designs of U-Net is the use of skip connections between the encoder and decoder, which helps to recover detailed information after upsampling. While most variations of U-Net adopt the original skip connection design, there is semantic gap between the encoder and decoder that can negatively impact model performance. Therefore, it is important to reduce this semantic gap before conducting skip connection. To address this issue, we propose a new segmentation network called FusionU-Net, which is based on U-Net structure and incorporates a fusion module to exchange information between different skip connections to reduce semantic gaps. Unlike the other fusion modules in existing networks, ours is based on a two-round fusion design that fully considers the local relevance between adjacent encoder layer outputs and the need for bi-directional information exchange across multiple layers. We conducted extensive experiments on multiple pathology image datasets to evaluate our model and found that FusionU-Net achieves better performance compared to other competing methods. We argue our fusion module is more effective than the designs of existing networks, and it could be easily embedded into other networks to further enhance the model performance. Our code is available at: `https://github.com/Zongyi-Lee/FusionU-Net`

Keywords Feature Fusion · Pathology Image Segmentation · Skip Connection · U-Net

1 Introduction

Medical imaging segmentation is a crucial area of AI research with great application value in areas such as computer aided diagnosis [1] and image-guided surgery [2] One of main chanllenges in this field is the lack of training data due to the fact that labeling medical images requires professional skills and also time-consuming. Pathology images, in particular, with many small and densely distributed target areas, present additional difficulties to segmentation tasks. As is pointed out by many researches, right inductive bias could help the model to generalize well on restricted training dataset [3][4]. While the inductive biases of Convolutional Neural Networks(CNNs) are locality and weights sharing, which are consistent with fact that for pathology images many features worth noticing are strongly locally related. In fact, CNNs do become dominant in such areas, and U-Net [5] is a specially successful one among numerous CNNs. U-Net is a typical encoder-decoder structure network, the shallow layers in the encoder part mainly work on capturing low-level features and the spatial semantic information grows richer as the layer progresses deeper. In the decoder part, upsampling is applied to restore the image to its full size, while skip connections are employed to combine coarse-grained features from deep layers with fine-grained features from shallow layers to aid in object details recovery. This design has led to U-Net's great success on numerous segmentation tasks and has also inspired many researches. However, most of these studies have only focused on improving the encoders or decoders but not altering the original skip connection design.

Recently, researchers have noticed the semantic gap between the encoder and decoder [6], and [7] carefully examined the contribution of different skip connections in U-Net and found that simple skip connections may not always be helpful and sometimes could even harm model performance. Based on this finding, they proposed a CCT module to fuse different feature maps of skip connections. Their fusion method mainly focuses on channel-wise information but

disregards the spatial relevance between adjacent layer outputs. Tracing back to the forward process of U-Net, it is evident that convolutions are the dominant computing operations, while the characteristic of convolutions guarantees the feature maps before and after convolutions are strongly locally relevant. With above analysis, it is natural to deduce that one of the keys to bride the semantic gap among different layer outputs is to accurately capture the local relevance. To this end, we propose a new network called FusionU-Net, which uses U-Net as base structure and adopts a fusion module to apply feature fusion on skip connections.

Unlike the design of previous works, we carefully considered the *relevance of adjacent skip connections* and implemented a different approach for the feature fusion. Our fusion design is based on the following considerations: 1) The feature maps produced by the deep and shallow layers of the encoder are inherently different while adjacent layer outputs have stronger relevance. Therefore, we only perform feature fusion between adjacent layers. 2) Our model should enable the information to be exchanged between any two encoder layer outputs. To achieve this we propose two-round fusion design. In the first round, we operate feature fusion between each pair of adjacent feature maps from shallow to deep encoder layers. In the second round, we operate in reverse order. This allows information to still be exchanged between feature maps with multiple layers in between, even though they are not explicitly fused. Additionaly the two-round design also enables the information to be switched bi-directionally. 3) The feature map of adjacent encoder layers are locally relevant, and the locality is also important characteristic of pathology images, thus we design a new method to fuse adjacent two feature maps together with fully considerations about keeping the feature map local adjacency, the details of which will be discussed in later section.

Our model has a clear and simple structure and requires significantly fewer training parameters compared with other state-of-the-art methods. To test our model, we conduct extensive experiments on three datasets and results strongly supports the superiority of our model. We argue that our fusion design represents a more effective and reasonable way and our fusion module could be easily embedded into other networks to further boost the performance of segmentation.

2 Related Works

2.1 U-Net based Networks

As various studies and application results having proved the effectiveness of U-Net design, many networks base on U-Net have been proposed. H-DenseUNet [8] is a typical U-Net variation that learns from DenseNet [9], it incorporates a hybrid feature fusion(HFF) layer to fuse 2D and 3D features and achieves impressing results on liver segmentation task. [10] designs R2U-Net, it employs U-Net as the base structure and applies recurrent residual block in decoder part for performance improvement. AttentionU-Net [11] aims at suppressing irreverent regions by utilizing a attention gate module, the attention gate could effectively highlight specific local features while introducing acceptable extra costs. ResU-Net [12] uses residual units to make it easier to train deeper networks. Based on ResU-Net, [13] adopted some new technologies such as squeeze and excitation blocks [14], Atrous Spatial Pyramidal Pooling(ASPP) [15] and came up with a new model called ResU-Net++. Recently, with the great success of Vision Transformer(ViT) [16] and Swin-Transformer [17], people have started to recognize the potential of Transformer on computer vision tasks. TransUNet proposed by [18] is the first model applying Transformer on U-Net structure for medical segmentation task, and they also use CNNs to extract low-resolution features since they believe the Transformer lay too much attention on global texture and tends to lack detailed localization information. Later proposed Swin-UNet [19] is a pure Transformer-based U-Net like network and it keeps the skip connections between the encoder and decoder.

2.2 Modification on skip connections

The aforementioned works primarily focus on the modifying encoder or decoder modules of U-Net in order to enhance the ability of feature extraction. However, they ignore the fact that as a key part of U-Net design, better processed skip connections could also greatly assist the model performance. [6] noticed the semantic gap between the encoder and decoder, and they chose to use ResPath to enhance skip connection to alleviate the gap. But their ResPath is operated for each skip connection individually, not considering exchanging information between layers. Despite the design deficiencies, their work pointed out that the original skip connection is not a perfect solution, and there is still much room for further improvement. UNet++ [20] also considers reorganizing skip connections. They apply a series of nested dense convolutions as skip pathways to communicate between encoder and decoder sub-networks. However, they did not realize the importance of fully exchange information between skip connections, and in their network the information could only passed from deep layers up to shallow layers and the information exchange is in single direction. [7] thoroughly studied the effect of each skip connection of U-Net and found that not every skip connection benefits the model performance. With these findings, they came up with UCTransNet, which is a U-Net shaped network embedded with a fusion module. The fusion module helps to exchange information among all feature maps produced by the encoder before conducting skip connection. In their CCT fusion module, the different feature maps produced
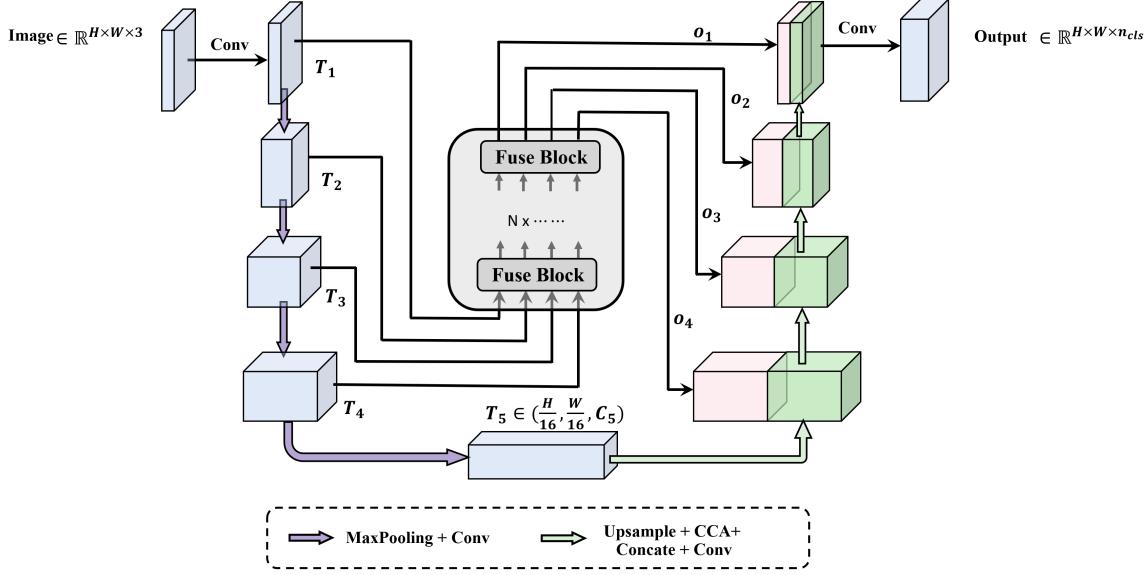
Figure 1: An overview of FusionU-Net structure

by encoder layers are combined together and then channel-wise attention is applied to exchange information between the combined map and each single feature map. We argue this design has two main shortcomings: Firstly, combining all feature maps together forms a giant feature map and it brings much greater computation cost to fusing operations; Secondly, the feature maps from very deep layers and from very shallow layers are intrinsically different, and we may not expect to gain much by fusing them.

Though the designs of fusion module from previous works are defective, they inspired us for the direction to further improve fusion design. And based on that we propose FusionU-Net, which contains the fusion module better handles the problems we've discussed above.

3 Model Description

In this section, we describe our proposed FusionU-Net in detail. Figure 1 illustrates the overview of our model. In essence, our model is a U-Net-shaped network that incorporates a fusion module to strengthen the skip connections. The whole structure can be divided into three parts: the encoder part, the fusion module part and the decoder part. In the following sections, we will thorough illustrate the details of these parts.

3.1 Encoder and Decoder

To ensure fairness and facilitate future comparison with other baseline models, as well as to evaluate the effectiveness of our fusion module, we have adopted a similar encoder and decoder design to UNet and it is consistent with UCTransNet [7].

The encoder is composed of 1 stem convolution block and 4 DownBlocks. Each DownBlock contains two convolution layer and a MaxPooling layer. For each DownBlock, the height and width of the feature map will shrink to half of its original size while the number of channels is doubled. The 4 outputs T_1, T_2, T_3, T_4 which are from the stem convolution block and the following three DownBlocks will be passed into the Feature Fusion module for further process.

The decoder recovers the feature map from the encoder to the original size with the help of 4 UpBlocks. The UpBlock will use bilinear interpolation for upsampling and then apply CCA module proposed by UCTransNet to compute channel attention together with feature map from skip connection. After that the two feature maps will be concatenated and passed to a convolution layer. At the final phase, a 1×1 convolution is used to transfer the channel number into the number of classes as the final segmentation results.
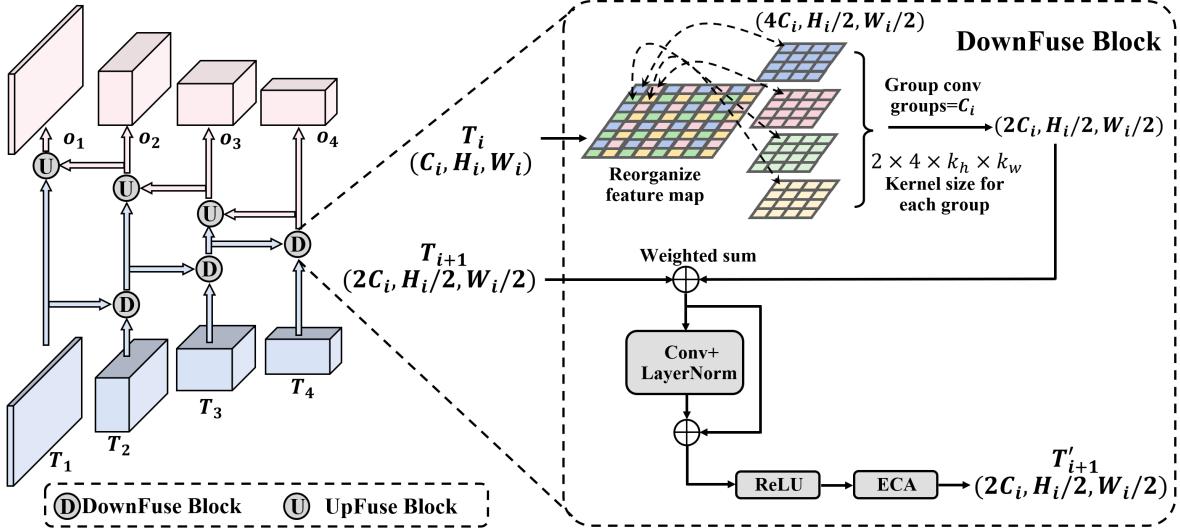
3

Figure 2: The structure of Fuse Block and DownFuse Block. The left part is Fuse Block structure while the right part represents the details of DownFuse Block

3.2 Feature Fusion Module

As previously discussed, the semantic information of feature maps from shallow layers and deep layers are vastly different. Therefore we choose to conduct feature fusion for each two feature maps from adjacent encoder outputs. Our fusion module is composed by stacking FuseBlocks, each FuseBlock consists of DownFuse blocks and UpFuse blocks as is shown in Figure 2. Noticed that the structures of UpFuse block and DownFuse block are similar thus we only represent the DownFuse block structure here. Both DownFuse and UpFuse blocks handle two adjacent skip connection feature maps and fuse them together. The entire fusion process is divided into two rounds, feature fusion is only conducted between two adjacent feature maps in one direction within each round. This can be either from top encoder layers to bottom encoder layers or the inverse way. More specifically, we firstly operate downward feature fusion on (T_1, T_2), (T_2, T_3) and finally (T_3, T_4), then in the opposite direction, we operate upward feature fusion on (T_4, T_3), (T_3, T_2) and (T_2, T_1) respectively. When doing feature fusion between T_3 and T_4, T_3 has already exchanged information with T_2 which has also combined features from T_1, thus information from T_1 could be indirectly passed to T_4. The second round of feature fusion aims to enable information to be transferred back into the shallow layers such that the changes of T_4 could be perceived by T_1 and this helps to achieve a bi-directional information transfer.

3.2.1 DownFuse Block

The DownFuse block takes the feature map from two adjacent encoder output feature maps, then fuse them and produce a feature map with the same size as the one with higher channel number. For example, we use T_i and T_{i+1} to represent the feature maps of two adjacent encoder output, and their shapes are (C_i, H_i, W_i) and $(2C_i, H_i/2, W_i/2)$. To fuse them together, we first transfer T_i into the same shape as T_{i+1}, then combine the two featue maps into one and apply several computing modules to further fuse the features. The complete working process can be described as follows:

1 We conduct feature map reorganization to transfer T_i into $(4C_i, H_i/2, W_i/2)$: The original feature map could be viewed as multiple 2-dimensional feature map stacked in channel-wise, and for each 2-D feature map, we sample the pixels with an interval of distance 1 horizontally and vertically, thus it is divided into 4 sub-graphs with half of original height and width. After that we stack these 4 sub-graphs at the channel dimmension, then we transfer a feature map from shape $(1, H_i, W_i)$ into $(4, H_i/2, W_i/2)$. For each channel of T_i, we apply above operations and then we get T_i with shape $(4C_i, H_i/2, W_i/2)$. The key of this design is that, unlike Pooling operations, we changed the feature map size without information loss. Furthermore, we also reserve the locality of previous feature map: the originally spatial neighboring 4 pixels now is still adjacent in channel-wise, in other words, *we transfer the spatial adjacency into channel adjacency*.

2 We apply group convolution with number of output channels set to $2C_i$ and number of groups set to C_i to transfer T_i into shape $(2C_i, H_i/2, W_i/2)$ which is exactly the shape of T_{i+1}. Notice that the kernel size of

Models	Params	Flops	MoNuSeg		GlaS	
	(M)	(G)	Dice(%)	IoU(%)	Dice(%)	IoU(%)
U-Net	14.75	25.18	76.51 ± 2.54	63.13 ± 3.15	86.42 ± 1.54	76.92 ± 1.47
U-Net++	9.16	26.72	77.83 ± 2.16	63.72 ± 2.92	88.02 ± 1.95	81.30 ± 1.50
SwinU-Net	27.14	5.91	77.85 ± 2.20	64.00 ± 1.95	84.84 ± 1.70	75.43 ± 2.15
TransU-Net	93.23	24.67	76.91 ± 1.95	62.33 ± 2.49	90.29 ± 0.92	82.97 ± 1.39
UCTransNet	66.24	32.98	79.17 ± 2.34	65.91 ± 2.85	89.70 ± 1.41	82.04 ± 2.12
ours	25.80	55.95	$\mathbf{80.04 \pm 1.38}$	$\mathbf{66.38 \pm 2.52}$	$\mathbf{91.05 \pm 1.65}$	$\mathbf{83.23 \pm 2.03}$

Table 1: The comparison with other models on MoNuSeg and GlaS datasets. For MoNuSeg and GlaS datasets we report three times of five fold cross validation results with form 'mean $\pm$ std'. The params and flops are calculated with input shape $1 \times 3 \times 224 \times 224$

Models	Neoplastic	Inflammatory	Connective	Dead	Non-Neopla	Average
UNet	73.09	56.73	57.12	19.49	56.78	52.64
UNet++	73.25	57.02	60.58	20.75	63.79	55.07
SwinUNet	71.57	54.62	56.41	19.86	56.48	51.79
TransUNet	**76.98**	57.77	61.44	24.24	**68.62**	**57.81**
UCTransNet	74.59	56.51	**61.81**	22.72	67.67	56.66
ours	75.37	**58.29**	60.71	**24.32**	67.78	57.29

Table 2: Comparison of different models on PanNuke dataset.

     convolution for each group will be $2 \times 4 \times k_h \times k_w$, thus the channel-wise pixels involved in the convolution are exactly the previously four adjacent pixels, and through this way locality of feature map is still well reserved and the computation cost also decreased vastly compared with normal convolution.

3 After making the two feature map to have same shape, we fuse them into one by a weighted sum.

4 The combined feature map from stage 3 is process by a convolution layer and an ECA layer [21] to better fuse and learn spatial and channel information.

3.2.2 UpFuse Block

The UpFuse block is pretty similar with the DownFuse block, we also firstly transfer the two feature maps into same shape and combine them together by weighted summation, then feeding the feature map into a convolution layer and an ECA layer. The only difference is that for UpFuse, we transfer the feature map with smaller spatial size into larger size by doing the inverse operation as the re-organize operation in DownFuse, and the rest procedure is basically the same.

4 Experiments

4.1 Datasets

We apply MoNuSeg [22], GlaS [23] and PanNuke [24] datasets to evaluate our model. The MoNuSeg datasets consits of 44 images, 30 for training and 14 for testing. The GlaS dataset has 85 images for training and 80 for testing. Compared with MoNuSeg and GlaS, PanNuke is a much more challenging task: PanNuke consists of exhaustible labels from 19 different tissues, and the 7904 images are randomly sampled from more than 20K whole slide images at different magnifications from multiple data sources.

4.2 Implementation Details

We train and test our model with PyTorch on a Nvidia 3090 GPU with 24 GB memory. For MoNuSeg and GlaS datasets we follow the setting in [7] and set the batch size as 4, and for PanNuke dataset the batch size is set to 16. Notice that images are all resized into 224×224 before feeding into the network. We also use simple image flip and rotation

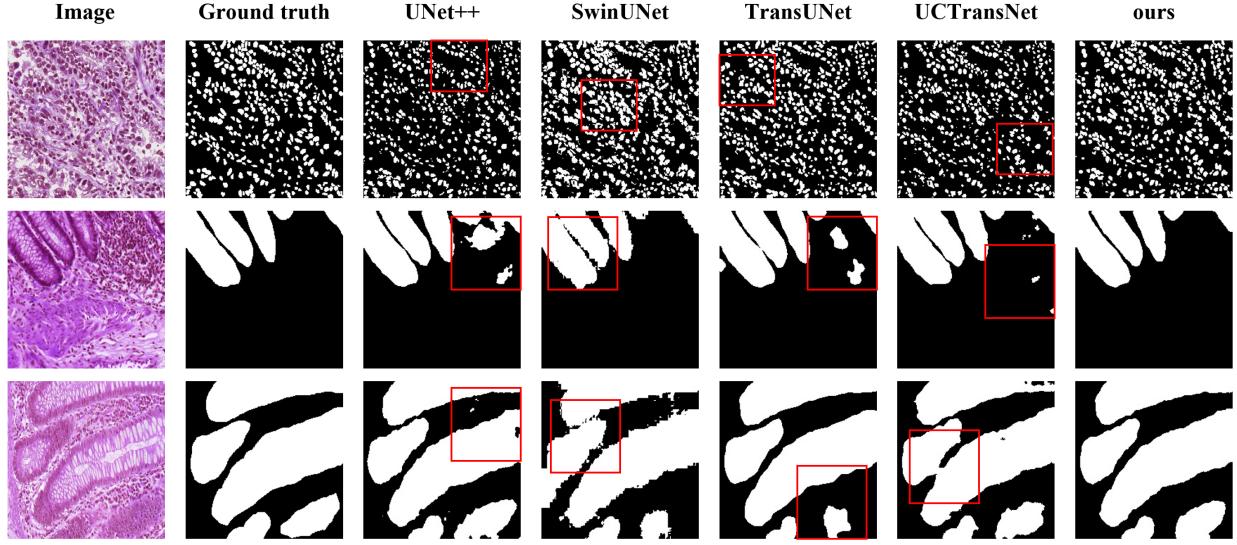| Image	Ground truth	UNet++	SwinUNet	TransUNet	UCTransNet	ours

Figure 3: Segmentation results on MoNuSeg and GlaS datasets
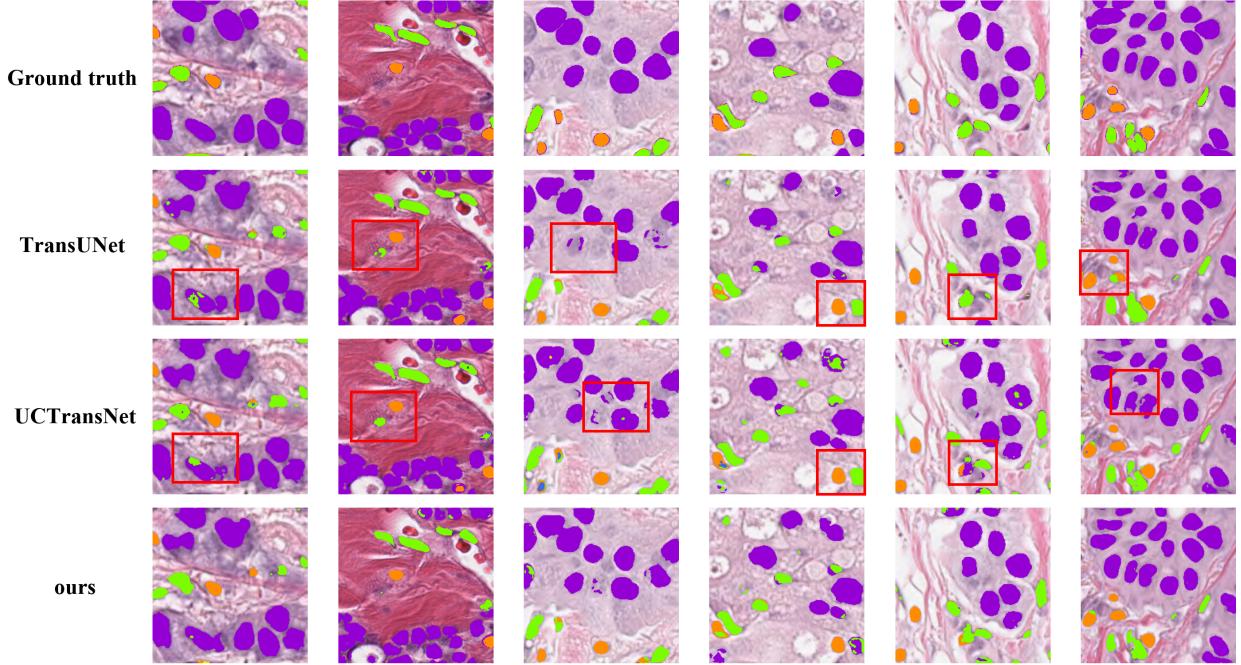

Figure 4: Segmentation results on PanNuke dataset

for data augmentation. As for loss functions, we employ cross entropy loss and dice loss on MoNuSeg and GlaS datasets, and for PanNuke, focal loss is applied to alleviate the adverse impact of imbalanced distribution of different labels. The learning rate scheduler of cosine annealing warm-up restart is employed to avoid getting stucked in local optimal too early. For MoNuSeg and GlaS, due to the limited number of training materials, we apply three times 5-fold cross-validation and average 15 results of all folds as the final value to make the results more convincing. For PanNuke dataset, we split the whole dataset into training set, validation set and test set with ratio 7:1:2. The model with best performance on validation set is chosen for final testing. For all models we do not use any pretrained-weights and directly initialize the weights before training the model. Dice coefficients and IoU are reported on MoNuSeg and GlaS as evaluation metrics, and for PanNuke we report the mean dice and dice coefficents of all 5 labels.

6

Method	MoNuSeg		GlaS		PanNuke
	Dice	IoU	Dice	IoU	(mean Dice)
No Fusion	76.51	63.31	86.42	77.08	53.82
Only Downward	76.95	63.27	86.96	78.23	54.54
Only Upward Fuse	77.87	64.51	88.42	79.12	55.75
DownFuse + UpFuse	**78.12**	**64.73**	**89.73**	**80.53**	**57.29**

Table 3: Ablation study about the effectiveness of DownFuse block and UpFuse block

Method	MoNuSeg		GlaS		PanNuke
	Dice	IoU	Dice	IoU	(mean Dice)
Pooling+Conv	77.49	63.81	88.95	80.02	56.89
Reorganize+Group-Conv	**78.12**	**64.73**	**89.73**	**80.53**	**57.29**

Table 4: Ablation study about the effectiveness of reorganize + group convolution

4.3 Comparison with other state-of-the-arts

To fully evaluate model performance, we compare our model with other state-of-the-art methods: UNet++ [20], UCTransNet [7], TransUNet [18] and SwinUNet [19]. For fairness, the code and settings of other models are kept consistent with those from publicly realeased resources. Table 1 reports the performance of all models on MoNuSeg and GlaS datasets, the results strongly prove that our model outperforms the others. Table 2 shows the results on PanNuke datasets, from which a similar conclusion could also be drawn. It is evident that our model achieves better predicting accuracies with relatively less training parameters. This success can be attributed to the better handling of skip connection. As discussed earlier, previous works like TransUNet and SwinUNet place too much emphasis on enhancing the encoder/decoder, these designs do help to improve the accuracy but the limits of naive skip connections constrain for further performance improvement. Other works like UNet++ try to enhance the skip connections part, they cannot achieve fully information exchange between skip connections because of the information flow is in single-direction. UCTransNet applies attention mechanism on each single and the combined feature maps to address that issue, but it introduces large number of extra training parameters and loses the local relevance. These problems are effectively dealt with by our fusion module, as evidenced by the experiment results. People may notice from the table that our model has relatively higher FLOPs, but this does not necessarily mean the model runs slower. We have conducted tests on the inference speed and found that our model reaches 48.24 fps, which is faster than UCTransNet with 41.60 fps. The increased FLOPs are primarily attributable to the dense convolution employed for fusing feature maps from deep layers, and it is our future work to address this unintended consequence with improved handling.

On PanNuke dataset our model also achieves favorable results, though the average dice seems to be slightly inferior to TransUNet, this is mainly due to the difference of the encoder. Our FusionU-Net primarily focus on fusing features across skip connections, and we utilize a relative simple encoder. In contrast, TransUNet places great emphasis on the encoder design and apply dense Transformer blocks to extract information on the final encoder layer, resulting in the network to be a nearly 4 times the size of our FusionU-Net. For complex tasks like PanNuke, the encoder has become the bottleneck and constrained the performance of our model. From a different perspective, our model's ability to achieve equivalent performance with a basic encoder and limited parameters proves the effectiveness of our fusion module, and this could be further supported by the comparison with other models like UCTransNet and UNet++.

4.4 Analytical Study

We have also conducted ablation studies to test the effectiveness of our module design and evaluate the model under various settings. These studies includes: 1) the contribution of DownFuse and UpFuse blocks 2) the effectiveness of re-organize + group convolution compared with Pooling + convolution;

Contribution of DownFuse and UpFuse: To prove the value of two-round fusion, we change the originial FuseBlock into one round fusion with either DownFuse or UpFuse and we also test for directly using the raw skip connection to show the necessity of doing feature fusion(notice we still use CCA for decoder part feature fusion under these settings). The experiment result is presented in table 3, and it demonstrates that the fusing operation before the skip connections is a useful way to enhance model performance. And we could observe that applying upward fusion helps more than downward fuse. This is because the original U-Net encoder forward process can also be viewed as a similar progress

with our downward fusion, thus the upward feature fusion which assists in passing the message from bottom back to top layers enable the model to better exchange information between layers. And it is also worth pointing out that even though downward fuse helps little alone, combining it with upward fuse will benefit a lot to the model just as the data shows.

Effectiveness of Reorganize and Group-conv: To keep the local adjacency and avoid information loss during the downsampling and upsampling process, we propose a better alternative by reorganizing pixels of the feature map and applying group convolution. To show the advantage of this method, we substitute the reorganize and group convolution with Pooling and a normal convolution and test the performance on three datasets. The new model's number of training parameters and flops grows into 34.98M and 97.15G, while the segmentation performance dropped as in shown in table 4. Therefore, it is evident that our design is superior to the traditional way.

5 Conclusion

U-Net is a highly effective model for pathology image segmentation and has inspired numerous works. In this paper, we aim to explore a different perspective on improving segmentation accuracy by modifying the original skip connection design. Our proposed network, FusionU-Net, is similar to U-Net but with an additional fusion module that applies feature fusion on skip connections. The fusion module is based on a two-round design to better handles the relevance of adjacent encoder outputs and enables information to be fully exchanged between any two skip connection feature maps. Additionally, we propose a new way of upsampling and downsampling by reorganizing the feature map and applying a group convolution. This approach can avoid information loss and preserve the pixel adjacency relationship effectively, which is particularly suitable for pathology images. Through extensive experiments and in-depth analysis, we demonstrate that our model is highly effective and our fusion module represents a superior method for fusing feature maps from skip connections.

Acknowledgments

References

[1] Dan You, Pengcheng Xia, Qiuzhu Chen, Minghui Wu, Suncheng Xiang, and Jun Wang. Autokary2022: A large-scale densely annotated dateset for chromosome instance segmentation. *arXiv preprint arXiv:2303.15839*, 2023.

[2] Syed Muhammad Anwar, Muhammad Majid, Adnan Qayyum, Muhammad Awais, Majdi Alnowami, and Muhammad Khurram Khan. Medical image analysis using convolutional neural networks: a review. *Journal of medical systems*, 42:1–13, 2018.

[3] Anirudh Goyal and Yoshua Bengio. Inductive biases for deep learning of higher-level cognition. *Proceedings of the Royal Society A*, 478(2266):20210068, 2022.

[4] Robert Geirhos, Patricia Rubisch, Claudio Michaelis, Matthias Bethge, Felix A Wichmann, and Wieland Brendel. Imagenet-trained cnns are biased towards texture; increasing shape bias improves accuracy and robustness. *arXiv preprint arXiv:1811.12231*, 2018.

[5] Olaf Ronneberger, Philipp Fischer, and Thomas Brox. U-net: Convolutional networks for biomedical image segmentation. In *Medical Image Computing and Computer-Assisted Intervention–MICCAI 2015: 18th International Conference, Munich, Germany, October 5-9, 2015, Proceedings, Part III 18*, pages 234–241. Springer, 2015.

[6] Nabil Ibtehaz and M Sohel Rahman. Multiresunet: Rethinking the u-net architecture for multimodal biomedical image segmentation. *Neural networks*, 121:74–87, 2020.

[7] Haonan Wang, Peng Cao, Jiaqi Wang, and Osmar R Zaiane. Uctransnet: rethinking the skip connections in u-net from a channel-wise perspective with transformer. In *Proceedings of the AAAI conference on artificial intelligence*, volume 36, pages 2441–2449, 2022.

[8] Xiaomeng Li, Hao Chen, Xiaojuan Qi, Qi Dou, Chi-Wing Fu, and Pheng-Ann Heng. H-denseunet: hybrid densely connected unet for liver and tumor segmentation from ct volumes. *IEEE transactions on medical imaging*, 37(12):2663–2674, 2018.

[9] Gao Huang, Zhuang Liu, Laurens Van Der Maaten, and Kilian Q Weinberger. Densely connected convolutional networks. In *Proceedings of the IEEE conference on computer vision and pattern recognition*, pages 4700–4708, 2017.

[10] Md Zahangir Alom, Mahmudul Hasan, Chris Yakopcic, Tarek M Taha, and Vijayan K Asari. Recurrent residual convolutional neural network based on u-net (r2u-net) for medical image segmentation. *arXiv preprint arXiv:1802.06955*, 2018.

[11] Ozan Oktay, Jo Schlemper, Loic Le Folgoc, Matthew Lee, Mattias Heinrich, Kazunari Misawa, Kensaku Mori, Steven McDonagh, Nils Y Hammerla, Bernhard Kainz, et al. Attention u-net: Learning where to look for the pancreas. *arXiv preprint arXiv:1804.03999*, 2018.

[12] Zhengxin Zhang, Qingjie Liu, and Yunhong Wang. Road extraction by deep residual u-net. *IEEE Geoscience and Remote Sensing Letters*, 15(5):749–753, 2018.

[13] Debesh Jha, Pia H Smedsrud, Michael A Riegler, Dag Johansen, Thomas De Lange, Pål Halvorsen, and Håvard D Johansen. Resunet++: An advanced architecture for medical image segmentation. In *2019 IEEE International Symposium on Multimedia (ISM)*, pages 225–2255. IEEE, 2019.

[14] Jie Hu, Li Shen, and Gang Sun. Squeeze-and-excitation networks. In *Proceedings of the IEEE conference on computer vision and pattern recognition*, pages 7132–7141, 2018.

[15] Liang-Chieh Chen, George Papandreou, Florian Schroff, and Hartwig Adam. Rethinking atrous convolution for semantic image segmentation. *arXiv preprint arXiv:1706.05587*, 2017.

[16] Alexey Dosovitskiy, Lucas Beyer, Alexander Kolesnikov, Dirk Weissenborn, Xiaohua Zhai, Thomas Unterthiner, Mostafa Dehghani, Matthias Minderer, Georg Heigold, Sylvain Gelly, et al. An image is worth 16x16 words: Transformers for image recognition at scale. *arXiv preprint arXiv:2010.11929*, 2020.

[17] Ze Liu, Yutong Lin, Yue Cao, Han Hu, Yixuan Wei, Zheng Zhang, Stephen Lin, and Baining Guo. Swin transformer: Hierarchical vision transformer using shifted windows. In *Proceedings of the IEEE/CVF international conference on computer vision*, pages 10012–10022, 2021.

[18] Jieneng Chen, Yongyi Lu, Qihang Yu, Xiangde Luo, Ehsan Adeli, Yan Wang, Le Lu, Alan L Yuille, and Yuyin Zhou. Transunet: Transformers make strong encoders for medical image segmentation. *arXiv preprint arXiv:2102.04306*, 2021.

[19] Hu Cao, Yueyue Wang, Joy Chen, Dongsheng Jiang, Xiaopeng Zhang, Qi Tian, and Manning Wang. Swin-unet: Unet-like pure transformer for medical image segmentation. In *Computer Vision–ECCV 2022 Workshops: Tel Aviv, Israel, October 23–27, 2022, Proceedings, Part III*, pages 205–218. Springer, 2023.

[20] Zongwei Zhou, Md Mahfuzur Rahman Siddiquee, Nima Tajbakhsh, and Jianming Liang. Unet++: Redesigning skip connections to exploit multiscale features in image segmentation. *IEEE transactions on medical imaging*, 39(6):1856–1867, 2019.

[21] Qilong Wang, Banggu Wu, Pengfei Zhu, Peihua Li, Wangmeng Zuo, and Qinghua Hu. Eca-net: Efficient channel attention for deep convolutional neural networks. In *Proceedings of the IEEE/CVF conference on computer vision and pattern recognition*, pages 11534–11542, 2020.

[22] Neeraj Kumar, Ruchika Verma, Sanuj Sharma, Surabhi Bhargava, Abhishek Vahadane, and Amit Sethi. A dataset and a technique for generalized nuclear segmentation for computational pathology. *IEEE transactions on medical imaging*, 36(7):1550–1560, 2017.

[23] Korsuk Sirinukunwattana, Josien PW Pluim, Hao Chen, Xiaojuan Qi, Pheng-Ann Heng, Yun Bo Guo, Li Yang Wang, Bogdan J Matuszewski, Elia Bruni, Urko Sanchez, et al. Gland segmentation in colon histology images: The glas challenge contest. *Medical image analysis*, 35:489–502, 2017.

[24] Jevgenij Gamper, Navid Alemi Koohbanani, Ksenija Benes, Simon Graham, Mostafa Jahanifar, Syed Ali Khurram, Ayesha Azam, Katherine Hewitt, and Nasir Rajpoot. Pannuke dataset extension, insights and baselines. *arXiv preprint arXiv:2003.10778*, 2020.